J. Condensed Matter Nucl. Sci. 13 (2014) 432–442

Research Article

It is Not Low Energy – But it is Nuclear*

Pamela A. Mosier-Boss †

Research Laboratory of Electronics, Massachusetts Institute of Technology,Cambridge, MA 02139, USA

Abstract

In this communication, CR-39 track results obtained as a result of Pd/D co-deposition are discussed and criticisms of those results are addressed. Implications of the CR-39 results with reports of transmutation are explored.
 ISSN 2227-3123

Keywords: CR-39, Energetic particles, Pd/D co-deposition, Transmutation

1. Introduction

Anomalous effects observed in the Pd/D system include heat, helium-4, energetic charged particles, tritium, neutrons, gamma/X-ray emissions, and transmutation. It was later shown that the heat did not correlate with either neutrons or tritium [1]. Instead it was found that the heat correlated with helium-4 [2]. These results indicated that there were at least two channels – an aneutronic channel that produced heat (the so-called true Fleischmann–Pons effect) and another channel that favored formation of energetic charged particles, neutrons, and tritium. It was Swartz [3] who suggested that, by adjusting the experimental parameters, one could switch from one channel to the other.

In the Pd/D co-deposition process that was pioneered by Szpak, both the heat [4,5] and energetic particle [6,7] producing channels have been observed. The focus of this communication is on the experimental observations of energetic particles as detected using CR-39 solid-state nuclear track detectors (STNTDs). In particular, methods used to identify the charged particles are discussed. In addition, criticisms of the Pd/D co-deposition CR-39 results are addressed in this communication. The implications of these results on the nuclear processes occurring inside the Pd lattice are explored.

*This work was funded by the Defense Threat Reduction Agency.
†E-mail: pboss@san.rr.com

 ISSN 2227-3123

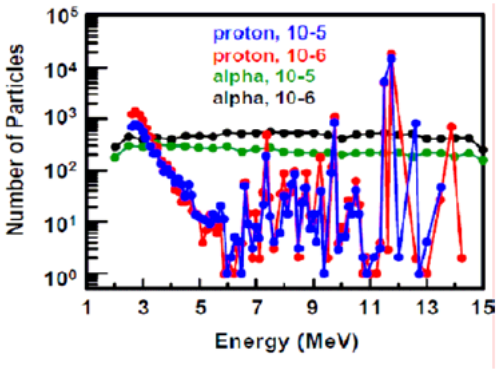

Figure 1. Results of LET spectrum analysis of the front side of CR-39 detectors 10-5 and 10-6 used in the SRI replication.

2. Summary of CR-39 Experimental Observations

2.1. Summary of Pd/D co-deposition results

The Stanford Research Institute (SRI) conducted several Pd/D co-deposition experiments that used CR-39 detectors. The experiments were conducted in the presence of a magnetic field. Two experiments were done with the detector inside the cell. In these experiments a 60 μm thick polyethylene film separated the Ag cathode from the detector. These detectors, identified as 10-5 and 10-6, underwent microscopic examination by our group. Tracks were observed on both sides of the detectors. These detectors were also scanned using an automated scanner.

Afterwards, the detectors were sent to Lipson and Roussetski. Using sequential etching, Lipson and Roussetski identified tracks due to 3 MeV protons as well as 12 and 16 MeV alphas [8]. Zhou of NASA subjected the scanned data to a linear energy transfer (LET) spectrum analysis [9]. The results, for the front side of detectors 10-5 and 10-6, are summarized in Fig. 1. From his analysis, Zhou concluded that there were 3–10 MeV protons as well as a continuum of alpha energies.

In another SRI experiment, The CR-39 detector was placed outside the cell. A 6 μm thick Mylar film was placed between the detector and the Ag cathode. The detector used in this experiment also underwent sequential etching analysis by Lipson and Roussetski. In their analysis, they identified proton recoil tracks due to 2.45 MeV (DD) neutrons.

Besides tracks due to energetic charged particles, triple tracks have also been observed in CR-39 detectors used in Pd/D co-deposition experiments. Triple tracks have not been observed in blank detectors or in detectors used in control experiments. These triple tracks are diagnostic of 14.1 MeV neutrons. Figure 2 shows a side-by-side comparison of a Pd/D co-deposition generated triple track and a similar DT neutron generated triple track. The top images were obtained by focusing the microscope optics on the surface of the detector. The bottom images are an overlay of two images taken on the surface of the detector and the bottom of the tracks. In both images, it can be seen that three tracks are breaking away from a center point.

2.2. Addressing the critiques of the Pd/D co-deposition CR-39 results

The three criticisms of the CR-39 results addressed in this communication are: (1) chemical damage vs. nuclear origins of the tracks; (2) why the Pd/D co-deposition tracks are predominantly circular is shape; and (3) the absence of Pd K-shell X-ray emissions that should simultaneously occur with the energetic charged particles.

A series of control experiments had been done to demonstrate that the tracks observed in CR-39 detectors used

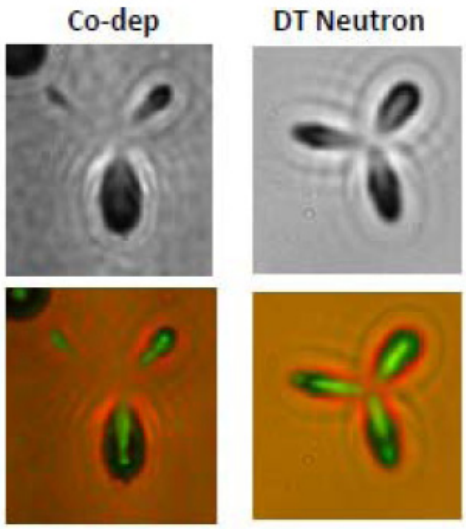

Figure 2. Microphotographs of Pd/D co-deposition and DT neutron generated triple tracks.

in Pd/D co-deposition experiments were not the result of chemical damage [6]. The most notable control experiment involved replacing $PdCl_2$ with $CuCl_2$. In both the $PdCl_2$ and $CuCl_2$ systems, the same chemical and electrochemical reactions are occurring. At the anode, oxygen and chlorine gases are evolved. At the cathode, metal plates out in the presence of evolving deuterium gas. Both Pd and Cu form dendritic metal deposits with a high surface area. The significant difference is that Pd absorbs deuterium and copper does not. Tracks in CR-39 were only observed in Pd/D co-deposition. This control experiment indicated that the tracks were not due to the dendrites piercing into the CR-39 or to localized production of hydroxide ions etching into the CR-39. Although the control experiments indicated that the tracks were not the result of chemical damage, these conclusions have been questioned. To address this, a Pd/D

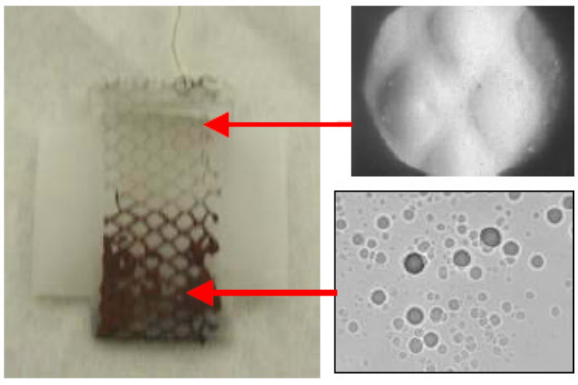

Figure 3. Ni/Au composite electrode used in a Pd/D co-deposition experiment and the resultant observations.

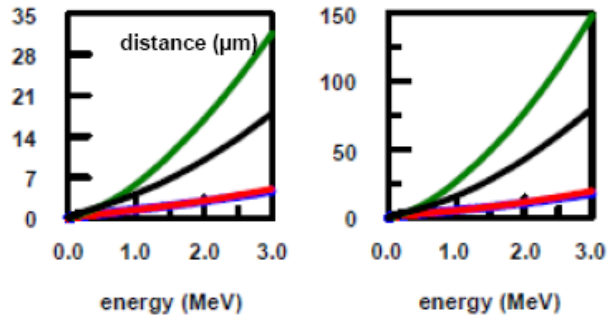

Figure 4. LET curves for protons (*green*), tritons (*black*), helium-4 (*blue*), and helium-3 (*red*) in palladium and water.

co-deposition experiment was conducted using a Ni/Au composite electrode, shown in Fig. 3.

Earlier it was shown that in the absence of an external E/B field, no tracks were obtained on a Ni screen cathode. Instead the impression of the Ni screen was observed on the CR-39 detector. For Au, Ag, and Pt cathodes, tracks were obtained in both the presence and absence of an external E/B field. In the composite cathode experiment, Au was electroplated on half of the Ni screen, as shown in Fig. 3. This composite cathode was placed in contact with a CR-39 detector and used in a Pd/D co-deposition experiment. At the end of the experiment, the detector was etched and analyzed. The results show that no tracks were obtained on the bare Ni half of the cathode. The impression of the Ni screen is observed. However, tracks were observed on the Au-coated Ni screen. Both halves of the cathode experienced the same chemical and electrochemical environment at the same time. If the pitting in CR-39 was due to chemical attack, those reactions would have occurred on both the bare Ni and Au-coated Ni halves of the cathode and both halves would have shown pitting of the CR-39 detector. But this was not observed. Therefore, the tracks observed in the CR-39 detectors are not the result of chemical attack.

The tracks observed in CR-39 detectors used in the Pd/D co-deposition experiments are predominantly circular in shape. After their birth, charged particles have to pass through the Pd lattice and a water layer before impinging upon the detector. LET curves were used to determine the magnitude of the effect of Pd and water on the energies of the particles. These LET curves, shown in Fig. 4, show that thin layers of Pd and water greatly slow down the

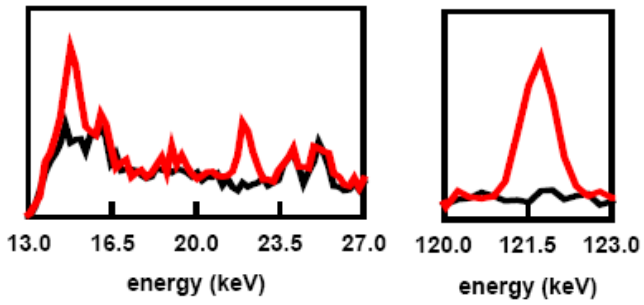

Figure 5. Gamma ray spectra of the lead cave obtained in the presence (*red*) and absence (*black*) of a ^{210}Po source.

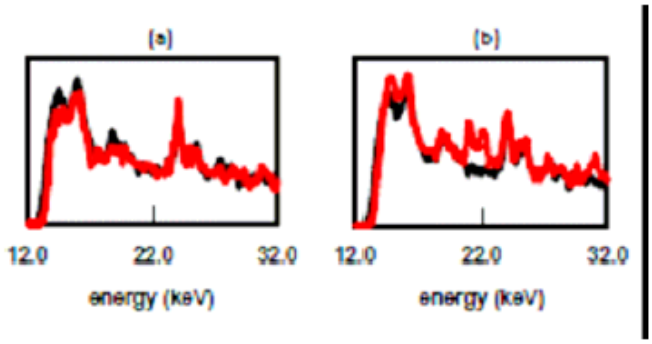

Figure 6. Gamma ray spectra obtained with the ^{210}Po–Pd sample (a) oriented perpendicular to the detector window and (b) facing the detector window. Background and sample spectra are in *black* and *red*, respectively.

charged particles. They also indicate that, CR-39 will only detect charged particles that are born near the surface of the Pd. Circular tracks indicate that the charged particles are entering perpendicular to the surface of the detector. These charged particles are the only ones with enough energy to get through the water layer to reach the detector. In one simulation, a CR-39 detector was exposed to an ^{241}Am source [10]. Placing 24 μm of Mylar between the detector and the ^{241}Am source slows the alphas by 4.41 MeV. The resultant tracks were primarily circular in shape and greatly resembled the tracks obtained as a result of Pd/D co-deposition.

It has been shown that X-rays are generated by the refilling of the K shell electron orbits ionized by the passage of charged particles. In 1989, Bennington et al. [11] and Deakin et al. [12] used SiLi detectors to detect these K-shell X-rays in Pd/D electrolysis experiments. No X-rays above background were detected. If the CR-39 is detecting charged particles, where are the concurrent Pd X-ray emissions? To address this apparent discrepancy, simulation experiments were conducted using a 0.1 μCi ^{210}Po source, a pure alpha particle emitter.

A CR-39 detector was exposed to the ^{210}Po source. The observed number of tracks was consistent for a 0.1 μCi source. A gamma-ray spectrum of the ^{210}Po source was obtained by placing the source inside the lead cave and pressed against the Be window of a HPGe detector. Figure 5 shows the time-normalized spectra obtained for the lead cave with and without the ^{210}Po source. From the spectra, it can be seen that three new gamma/X-ray lines at 14.8, 21.9, and 121.7 keV are present in the ^{210}Po source spectrum. As ^{210}Po is a pure alpha emitter, these new lines cannot be due to ^{210}Po. Both gamma rays and alpha particles will stimulate the K shell X-ray emission. While the presence of the contaminant in the ^{210}Po source was unexpected, it did present an opportunity to separate and quantify the alpha/gamma contributions in stimulating the Pd K shell X-rays.

The ^{210}Po source was placed in contact with a Pd foil. Spectra were obtained by placing the sample perpendicular to the Be window of the HPGe detector, Fig. 6(a), and directly facing the detector, Fig. 6(b). No Pd K shell X-rays were observed with the ^{210}Po-Pd sample facing away (perpendicular to) the detector. However, when the Pd foil and ^{210}Po source were facing the Be window of the HPGe detector, the Pd Kα line at 21.1 keV was observed as was the 21.9 keV line due to the contaminant in the ^{210}Po source. Consequently, the orientation of the cell relative to the HPGe detector will determine whether or not tracks will be observed.

Experiments were then conducted by placing 100 μm thick acrylic film between the Pd foil and the ^{210}Po source. The acrylic film will block the alphas from ^{210}Po but not the gammas from the unknown contaminant. Figure 7 summarizes the results. Figure 7(a) is the spectrum of the Pd foil in the lead cave. The fluorescence from the lead bricks is stimulating the Pd K shell X-ray emissions. Figure 7(b) is the spectrum obtained for the ^{210}Po source and shows

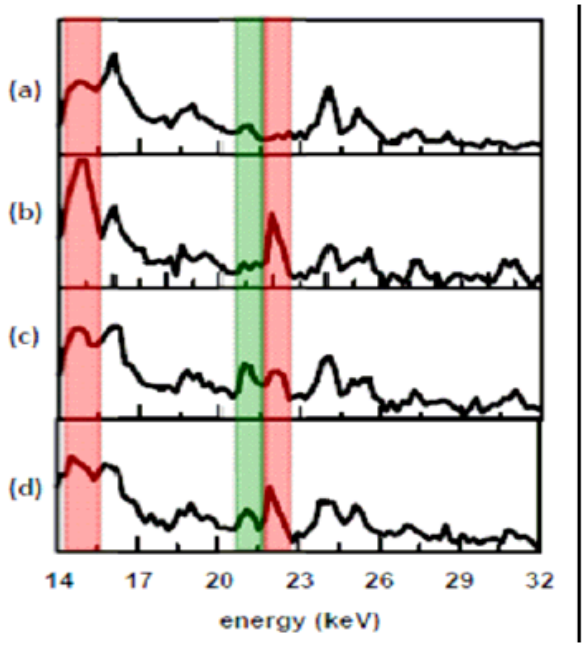

Figure 7. Summary of the ^{210}Po–Pd experiments where the red bars indicate the gamma lines of the unknown contaminant(s) and the green bar indicates the Pd K shell X-ray. Experiments were conducted by placing the samples in direct contact with the HPGe detector. (a) Pd foil in the lead cave, (b) ^{210}Po source, (c) Pd foil in contact with the ^{210}Po source, and (d) a 100 μm thick acrylic film is between the Pd foil and the ^{210}Po source.

the gamma lines due to the unknown contaminant(s). Figure 7(c) is the spectrum obtained when the ^{210}Po source is in contact with the Pd foil. The Pd K-shell emissions are stimulated by the lead cave background, the ^{210}Po alphas, and the gamma rays from the unknown(s). Figure 7(d) is the spectrum obtained when the 100 μm thick acrylic film is between the ^{210}Po source and the Pd foil. The Pd K-shell emissions are stimulated by the lead cave background and the gamma rays from the unknown(s). It is assumed that the background, ^{210}Po α-particle, and unknown contaminant γ-ray stimulations contribute additively to the Pd Kα emissions of the Pd–^{210}Po sample, Fig. 7(c). With this assumption, the estimated contributions of each source, in stimulating the Pd K shell X-ray emissions, are 35.2% due to background (lead fluorescence), 44.4% due to the ^{210}Po α-particles, and 20.4% due to the unknown contaminant gamma rays.

The results of the ^{210}Po–Pd experiments discussed *vide supra* can be used to determine whether or not Pd K shell X-rays should have been observed in the Pd/D co-deposition experiments. Figure 8(a) shows a photomicrograph of tracks obtained by scanning a CR-39 detector used in a Pd/D co-deposition experiment. The scanner identifies and numbers objects in the scanned image, Fig 8(b). Based upon measurements of object symmetry and contrast, the computer algorithm identifies tracks whose properties are consistent with those of nuclear generated tracks. Positively identified tracks are indicated by green rectangles, Fig. 8(c).

In a 1 mm $\times$ 20 mm area of the CR-39 detector, the total number of tracks positively identified by the scanner in this area was 1079. The scanner does not count overlapping tracks. To determine whether or not Pd K shell X-rays would have been observed in the experiment, it is assumed that the observed tracks are due to charged particle interactions with the detector and not neutrons. As shown in Fig. 8(c), the number of tracks in this one image is undercounted by a factor of $\sim$3. Therefore, at a minimum, the number of tracks is undercounted by a factor of 3. However, the charged

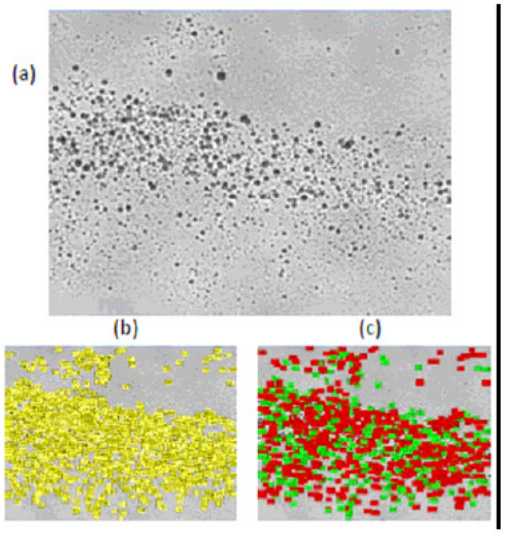

Figure 8. Scanned image of CR-39 detector used in a Pd/D co-deposition experiment: (a) raw image, (b) objects identified in the image, (c) after processing, identified tracks are *green*, non-tracks are *red*.

particle stimulation of the Pd K shell X-rays will occur throughout the Pd deposit. Ignoring absorption of the Pd K-shell X-rays by the Pd deposit and cell components, in the worst-case scenario, it is estimated that the charged particles are undercounted by a factor of 1000. The total area of the detector is 10 mm × 20 mm. Taking this larger area into account, the charged particles are estimated to be undercounted by a factor of 10 000. Therefore, in this worst-case scenario, the number of charged particles is 1.079×10^7. These experiments typically run for 2 weeks. For a two-week experiment (1.2096×10^6 s), the rate of particle production is estimated to be 8.9 particles s^{-1}.

Figure 7(a) and (d) is the time normalized spectra measured, in the Pb cave, for the Pd foil and for the experiment in which the 100 μm thick acrylic sheet was placed between the Pd foil and the ^{210}Po source. The measured peak areas for the line due to the Pd K-shell X-rays are tabulated in Table 1. From the data, the peak area, resulting from stimulation by the γ-rays from the unknown contaminant in the ^{210}Po source, is measured to be 5.31×10^{-5}. As discussed *vide supra*, the contribution of the unknown gamma contaminant to the Pd K-shell X-ray line is 20.4%. The ^{210}Po α-particles are responsible for 44.4% of the signal. A 0.1 μCi ^{210}Po α source will have 3700 decays s^{-1}. For the time-normalized spectra, this means that 3700 α particles will result in a Pd K-shell X-ray line with a peak area of 1.156×10^{-4}. In contrast, the increase in peak area of 8.9 charged particles, in the time-normalized spectrum, is calculated to be 2.8×10^{-7}. This is too small an increase in peak area to see in the measured spectrum. In addition, in this particular experiment, the cathode would have been oriented perpendicular to the HPGe detector. In this configuration, no Pd K-shell X-rays would have been observed, i.e. Fig. 6(a).

Measurement of K-shell X-rays occurs in real-time. In contrast CR-39 is an example of a constantly integrating detector, which means that when an event occurs, it is permanently stamped in the detector. The results discussed *vide supra* indicate that, although tracks significantly above background were observed in CR-39 detectors used in Pd/D co-deposition, the rate of charged particle production is too low to be detected by measuring the Pd K-shell X-ray emissions.

Table 1. Measured peak areas of the Pd Kα line shown in the time-normalized spectra in Fig. 7(a) and (d).

Sample	Area of Pd K-shell X-ray line	Cause of stimulation [a,b]
Pd foil	9.22×10^{-5}	b kg
^{210}Po-100 μm acrylic-Pd foil	1.453×10^{-4}	b kg + γ

[a]b kg is the background stimulation, γ is the gamma rays from the unknown contaminant(s) in the ^{210}Po source .
[b]The peak area resulting from stimulation by the unknown γ source is 5.31×10^{-5}.

2.3. Implications of the CR-39 results

In the absence of a magnetic field, the Pd deposit has a uniform "cauliflower"-like structure that consists of aggregates of spherical micro-globules. Figure 9(a) is an SEM microphotograph that shows the morphology of a Pd deposit that has been subjected to an external magnetic field. The Lorenz forces of the magnetic field have caused the Pd micro-globules to form the star-like features seen in Fig. 9(a). The development of these structural features in the magnetic field experiments requires high-energy expenditure.

EDX analysis of one of the spots is shown in Fig. 9(b). A very small peak due to Pd is observed. Larger peaks due to Fe, Cr, Ni, and Al are also observed. EDX detection limits are on the order of 0.1% [13]. Given the insensitivity of the EDX technique, the inhomogeneous distribution of the new elements, and the fact that the experiment was done using

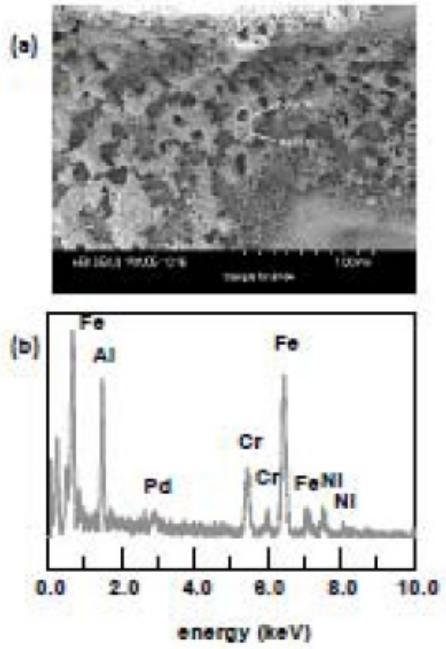

Figure 9. (a) SEM photomicrograph of the Pd deposit subjected to a magnetic field. (b) EDX analysis of one of the circled spots on the deposit.

a plastic cell, these new elements cannot be due to contamination. These same elements have been reported by others using a wide variety of conditions, e.g. different electrode materials and loading methods such as electrolysis, surface plasma electrolysis, gas pressure, plasma discharge, ion implantation, bubble collapse loading, and laser initiation [14]. But are the new elements observed the result of multi-body deuteron fusion or the disintegration of the Pd lattice? The energetic particles detected by solid-state nuclear track detectors such as CR-39 provide some insight as to the nature of the processes occurring inside the Pd lattice.

As discussed *vide supra,* the tracks in CR-39 used in Pd/D co-deposition experiments in the presence of a magnetic field were identified as being caused by 3–10 MeV protons, 2–15 MeV alphas, 2.45 MeV neutrons, and 14.1 MeV neutrons. Others have also reported detecting these energetic particles in their experiments. Roussetski [15] reported seeing triple tracks, which are diagnostic of 14.1 MeV, in his CR-39 experiments involving Pd/PdO:D heterostructures. Using CR-39 and Au/Pd/PdO:D heterostructures, Lipson et al. [16] reported seeing tracks due to 3 MeV protons and 1 MeV tritons. They also detected 2.5 MeV neutrons using NE213 detectors. In experiments using Si surface barrier detectors, including a dE-E telescope, Lipson et al. [17] detected 8–14 MeV alpha emissions from Au/Pd/PdO samples that had been loaded electrolytically with deuterium. Lipson et al. [18] conducted *in-situ* electrolysis experiments in which the Pd foil cathode was in direct contact with a CR-39 detector. Using Cu and Al spacers between the cathode and the detector, they identified the particles emitted as being 1.7 MeV protons and 11–16 MeV alphas.

The 2.45 MeV neutrons, 3–10 MeV protons, 14.1 MeV neutrons, and 1–7 MeV alphas can be accounted for by the following primary (1) and (2) and secondary fusion reactions (3) and (4):

$$\mathrm{D} + \mathrm{D} \rightarrow \mathrm{T}(1.01\ \mathrm{MeV}) + \mathrm{p}(3.02\ \mathrm{MeV}), \tag{1}$$

$$\mathrm{D} + \mathrm{D} \rightarrow \mathrm{n}(2.45\ \mathrm{MeV}) + {}^{3}\mathrm{He}\ (0.82\ \mathrm{MeV}), \tag{2}$$

$$\mathrm{D} + \mathrm{T}(\leq 1.01\ \mathrm{MeV}) \rightarrow \alpha(6.7 - 1.4\ \mathrm{MeV}) + \mathrm{n}(11.9 - 17.2\ \mathrm{MeV}), \tag{3}$$

$$\mathrm{D} + {}^{3}\mathrm{He}\ (\leq 0.82\ \mathrm{MeV}) \rightarrow \alpha(6.6 - 1.7\ \mathrm{MeV}) + \mathrm{p}(12.6 - 17.5\ \mathrm{MeV}). \tag{4}$$

The 7–16 MeV alphas can only come from another nuclear process. Fission reactions are known to produce these 'long-range alphas.' The EDX analysis of a cathode used in a magnetic field experiment, Fig. 9(b), shows that the peak due to Pd is significantly smaller than those for Fe, Al, Cr, and Ni. This implies that the Pd has been consumed. Both the sequential etching analysis and LET spectrum analysis of a CR-39 detector used in a magnetic field detector, discussed *vide supra*, showed the presence of long-range alphas. As the source of the long- range alphas is fission, it is very likely that the new elements seen in the EDX spectrum result from fissioning of the Pd nucleus.

3. Conclusions

In this communication, the use of microscopic examination, sequential etching, and LET spectrum analysis to identify the energetic charged particles and neutrons responsible for the tracks in CR-39 detectors used in Pd/D co-deposition experiments were discussed. These analytical techniques gave complementary results. The energetic particles were identified as 2.45 MeV neutrons, 3–10 MeV protons, 2–15 MeV alphas, and 14.1 MeV neutrons.

There have been questions/critiques about the Pd/D co-deposition CR-39 results. These have been addressed in this communication. In one criticism, the nuclear origin of the tracks has been questioned. Using a bare Ni, Au-plated Ni

screen composite cathode in a Pd/D co-deposition experiment, it was demonstrated that the observed pitting in CR-39 detectors were not the result of chemical damage. There have been questions as to why the Pd/D co-deposition tracks are predominantly circular in shape. LET curves for charged particles in Pd metal and water showed that only particles traveling perpendicular to the CR-39 detector have sufficient energy to impact the detector. As a result, the tracks are primarily circular in shape. It has been noted that charged particles traversing through a metal will stimulate K-shell X-rays. Yet these X-rays are not observed. Using a ^{210}Po source, it was shown that the experimental configuration determined whether or not X-rays would be seen. It was also shown that the rate of charged particle production was too low to detect measurable Pd K shell X-ray emissions.

The neutrons, protons, and 2–7 MeV alpha particles that have been detected in CR-39 used in Pd/D co-deposition have energies that are consistent with both primary and secondary fusion reactions. The alphas with energies between 7 and 15 MeV are referred to as long range alphas. These alphas have also been detected in CR-39 detectors used in Pd/D co-deposition reactions. The only known source of these long-range alphas is fission reactions. This suggests that the new elements observed on the cathodes are caused by fissioning of the Pd nucleus.

Currently within the CMNS community there has been disagreement as to what constitutes LENR. There are those in the community who contend that LENR is only heat and helium-4. Energetic particles with energies in the MeV range are clearly not low energy. However, they can only result from nuclear processes.

Acknowledgments

This communication is dedicated to the memory of Andrei Lipson. Replication of the co-deposition experiment by SRI is acknowledged as well as the sequential etching analysis of the detectors done by Lipson and Roussetski and the LET spectrum analysis done by Zhou. Steve Krivit of New Energy Times is acknowledged for organizing the SRI replication and subsequent analysis by Lipson and Roussetski. She is grateful for the support and encouragement she has received from both Frank Gordon and Dr. J.W. Khim. She also acknowledges thought provoking discussions she has had with Peter Hagelstein, Mitchell Swartz, Fran Tanzella, Roger Boss, Pat McDaniel, and Larry Forsley.

References

[1] J.O'M. Bockris, G.H. Lin, R.C. Kainthla, N.J.C. Packham and O. Velev, Does tritium form at electrodes by nuclear reactions? in *The First Annual Conference on Cold Fusion*. 1990. University of Utah Research Park, Salt Lake City, Utah: National Cold Fusion Institute.

[2] M.H. Miles, R.A. Hollins, B.F. Bush, J.J. Lagowski and R.E. Miles, Correlation of excess power and helium production during D_2O and H_2O electrolysis using palladium cathodes, *J. Electroanal. Chem*. **346** (1993) 99–117.

[3] M. Swartz, Three physical regions of anomalous activity in deuterated palladium, *Infinite Energy* **14** (2008) 19–31.

[4] S. Szpak, P.A. Mosier-Boss and J.J. Smith, On the behavior of Pd deposited in the presence of evolving deuterium, *J. Electroanal. Chem.* **302** (1991) 255–260.

[5] S. Szpak, P.A. Mosier-Boss, M.H. Miles and M. Fleischmann, Thermal behavior of polarized Pd/D electrodes prepared by co-deposition, *Thermochimica Acta* **410** (2004) 101–107.

[6] P.A. Mosier-Boss, S. Szpak, F.E. Gordon and L.P.G. Forsley, Use of CR-39 in Pd/D co-deposition experiments, *Eur. Phys. J. Appl. Phys*. **40** (2007) 293–303.

[7] P.A. Mosier-Boss, S. Szpak, F.E. Gordon and L.P.G. Forsley, Triple tracks in CRT-39 as the result of Pd–D co-deposition: evidence of energetic neutrons, *Naturwissenschaften* **96** (2009) 135–142.

[8] A.G. Lipson, A.S. Roussetski, E.I. Saunin, F. Tanzella, B. Earle and M. McKubre, Analysis of the CR-39 detectors from SRI's SPAWAR/Galileo type electrolysis experiments #7 and #5. Signature of possible neutron emission, 8^{th} *International Workshop on Anomalies in Hydrogen/Deuterium Loaded Metals*, pp. 182–203, October 2007.

[9] D. O'Sullivan, D. Zhou, W. Heinrich, S. Roesler, J. Donnelly, R. Keegan, E. Flood and L. Tommasino, Cosmic rays and dosimetry at aviation altitudes, *Radiation Measurement* **31** (1999) 579–584.

[10] P.A. Mosier-Boss, S. Szpak, F.E. Gordon and L.P.G. Forsley, Characterization if tracks in CR-39 detectors obtained as a result of Pd/D co-deposition, *Eur. Phys. J. Appl. Phys*. **46** (2009) 30901.
[11] S.M. Bennington, R.S. Sokhi, P.R. Stonadge, D.K. Ross, M.J. Benham, T.D. Beynon, P. Whithey, I.R. Harris and J.P.G. Farr, A search for the emission of X-rays from electrolytically charged palladium-deuterium, *Electrochimica Acta* **34** (1989) 1323–1326.
[12] M.R. Deakin, J.D. Fox, K.W. Kemper, E.G. Myers, W.N. Shelton and J.G. Skofronick, Search for cold fusion using X-ray detection, *Phys. Rev. C* **40** (1989) R1851–R1853. .
[13] http://www.web.pdx.edu/∼jiaoj/phy451/Lect7.pdf
[14] G. Miley and P.J. Shrestha, Review of Transmutation Reactions in Solids, *Condensed Matter Nuclear Science*, World Scientific, NewYork, pp. 361–378, 2006.
[15] A.S. Roussetski, Application of CR-39 plastic track detector for detection of DD and DT-reaction products in cold fusion experiments, 8^{th} *International Conference on Cold Fusion*, 2000.
[16] A.G. Lipson, B.F. Lyakhov, A.S. Roussetski, T. Akimoto, T. Mizuno, N. Asami, R. Shimada, S. Miyashita and A. Takahashi, Evidence for low-intensity D–D reaction as a result of exothermic deuterium desorption from Au/Pd/PdO:D heterostructure, *Fusion Technol*. **38** (2000) 238–252. .
[17] A.G. Lipson, B.F. Lyakhov, A.S. Roussetski and N. Asami, Evidence for DD-reaction and a long-range alpha emission in Au/Pd/PdO:D heterostructure as a result of exothermic deuterium desorption, 8^{th} *International Conference on Cold Fusion*, 2000.
[18] A.G. Lipson, A.S. Roussetski, G.H. Miley and C.H. Castano, In-situ charged particles and X-ray detection in Pd thin film-cathodes during electrolysis in Li_2SO_2/H_2O, 9^{th} *International Conference on Cold Fusion*, 2002.